Biophysical Journal
Article

Biophysical Society

2-ns Electrostimulation of Ca^{2+} Influx into Chromaffin Cells: Rapid Modulation by Field Reversal

Josette Zaklit,[1,*] Gale L. Craviso,[2] Normand Leblanc,[2] P. Thomas Vernier,[3] and Esin B. Sözer[3,*]
[1]Department of Electrical and Biomedical Engineering, College of Engineering, University of Nevada, Reno; [2]Department of Pharmacology, University of Nevada, Reno School of Medicine, Reno, Nevada; and [3]Frank Reidy Research Center for Bioelectrics, Old Dominion University, Norfolk, Virginia

ABSTRACT Cellular effects of nanosecond-pulsed electric field exposures can be attenuated by an electric field reversal, a phenomenon called bipolar pulse cancellation. Our investigations of this phenomenon in neuroendocrine adrenal chromaffin cells show that a single 2-ns, 16 MV/m unipolar pulse elicited a rapid, transient rise in intracellular Ca^{2+} levels due to Ca^{2+} influx through voltage-gated calcium channels. The response was eliminated by a 2-ns bipolar pulse with positive and negative phases of equal duration and amplitude and fully restored (unipolar-equivalent response) when the delay between each phase of the bipolar pulse was 30 ns. Longer interphase intervals evoked Ca^{2+} responses that were greater in magnitude than those evoked by a unipolar pulse (stimulation). Cancellation was also observed when the amplitude of the second (negative) phase of the bipolar pulse was half that of the first (positive) phase but progressively lost as the amplitude of the second phase was incrementally increased above that of the first phase. When the amplitude of the second phase was twice that of the first phase, there was stimulation. By comparing the experimental results for each manipulation of the bipolar pulse waveform with analytical calculations of capacitive membrane charging/discharging, also known as accelerated membrane discharge mechanism, we show that the transition from cancellation to unipolar-equivalent stimulation broadly agrees with this model. Taken as a whole, our results demonstrate that electrostimulation of adrenal chromaffin cells with ultrashort pulses can be modulated with interphase intervals of tens of nanoseconds, a prediction of the accelerated membrane discharge mechanism not previously observed in other bipolar pulse cancellation studies. Such modulation of Ca^{2+} responses in a neural-type cell is promising for the potential use of nanosecond bipolar pulse technologies for remote electrostimulation applications for neuromodulation.

SIGNIFICANCE Novel electrostimulation approaches for modulating the nervous system are actively being sought for clinical applications. Here, we introduce ultrafast modulation of Ca^{2+} influx into neuroendocrine adrenal chromaffin cells by single 2-ns unipolar and bipolar electric pulses. The Ca^{2+} response induced by a 2-ns unipolar pulse is absent in cells exposed to a 2-ns bipolar pulse and can be recovered by adding only a 30-ns interval between the two opposite polarity pulses. We characterized the modulation and explained the experimental results with theoretical calculations of capacitive membrane charging. The remarkable agreement between the theory and experiments can be used for predictive modeling of responses to this excitation modality, which has significant potential for remote electrostimulation.

INTRODUCTION

Electrical stimulation approaches for treating neurological and psychiatric disorders involve the use of both implantable (1,2) and noninvasive (3,4) technologies. Their successful use in the clinic has triggered a rapidly growing effort aimed at developing new approaches to modulate the nervous system. Electric pulses that are only nanoseconds in duration are included in this effort, and their potential application for neuromodulation is supported by the demonstration that trains of 12-ns pulses safely activate skin nociceptors (5) and continuously elicit action potentials in isolated peripheral nerves without damaging the nerve fibers (6). Highlighting their potential further for a variety of clinical applications is a recent report by Gianulis et al. (7) that introduced a new paradigm for noninvasive, focused electrostimulation that is based on delivering synchronized bipolar nanosecond pulses. The central premise of this paradigm is

Submitted July 22, 2020, and accepted for publication December 16, 2020.
*Correspondence: jelzaklit@unr.edu or esozer@odu.edu
Editor: Eric Sobie.
https://doi.org/10.1016/j.bpj.2020.12.017

that biological effects evoked by a nanosecond electric pulse can be cancelled or attenuated by immediately applying a second pulse of the opposite electric field polarity, a phenomenon called bipolar pulse cancellation. An example of how this can be applied for neuromodulation appears in the report by Casciola et al. (8) showing that a 200-ns pulse can trigger nerve excitation but not when the pulse is followed by another pulse of the opposite electric field polarity.

Bipolar pulse cancellation has been demonstrated for many cell types that include both excitable and nonexcitable cells, for pulse durations that range from 2 to 900 ns, and for diverse biological end points, one of which is electropermeabilization of the plasma membrane to ions and small nonpermeant dyes (9–16). Bipolar cancellation of changes in plasma membrane permeability was first described by Ibey et al. (9) in a report showing that Chinese hamster ovary cells exposed to a 600-ns bipolar pulse exhibit reduced Ca^{2+} influx and uptake of the dye propidium iodide as compared with the same total duration unipolar pulse. Around the same time, Pakhomov et al. (10) reported that electropermeabilization-induced Ca^{2+} influx into Chinese hamster ovary cells initiated by a 60- or a 300-ns unipolar pulse could be attenuated (partially cancelled) when each pulse was followed by the delivery of a second pulse of the same duration but with the opposite polarity. Similarly, plasma membrane electropermeabilization in U-937 cells, assessed by monitoring uptake of the dye YO-PRO-1 and efflux of the dye calcein, was reduced by a train of 2-ns bipolar pulses when compared with responses elicited by a train of 2-ns unipolar pulses (11). The parameters of the bipolar pulse that were determined to be important for a cancelling effect included the interval between the positive and negative phases of the pulse and the electric field amplitude of the reversed polarity phase (6,9–16).

The mechanism(s) responsible for bipolar pulse cancellation is still unknown. One plausible mechanism proposed to explain bipolar pulse cancellation is the accelerated membrane discharge hypothesis (10,11,15). This hypothesis assumes that the cell membrane is a simple capacitive electrical model that is charged during the first (positive) phase of the bipolar pulse, followed by accelerated discharge caused by fast reversal of the electric field during the negative pulse phase, thereby reducing the time over which the membrane potential is above a critical potential for permeabilization (11,15). Interestingly, the accelerated membrane discharge hypothesis has not yet been able to predict the experimental results obtained in the bipolar pulse cancellation studies (10,11,15).

For more than a decade, we have been assessing the potential for nanosecond electric pulses to modulate neural cell excitability, using neuroendocrine adrenal chromaffin cells as a model system (17–20). Chromaffin cells, best known as the cell type that mediates the "fight or flight" response by releasing catecholamines into the circulation, are considered a model of postganglionic sympathetic neurons (21). When exposed to a single 4-ns (17) or 5-ns pulse (18,19), the cells undergo a rapid rise in intracellular Ca^{2+} concentration ($[Ca^{2+}]_i$) that is mediated by influx of Ca^{2+} solely via voltage-gated Ca^{2+} channels (VGCCs), which in turn evokes the release of catecholamines via exocytosis (18). The mechanism responsible for VGCC activation and hence Ca^{2+} influx is consistent with Na^+-dependent membrane depolarization mediated by a reversible permeabilization of the cell membrane to Na^+ (19,22).

Initial studies investigating whether an electric field reversal could attenuate/cancel Ca^{2+} influx into chromaffin cells were carried in cells exposed to 150-ns unipolar and bipolar electric pulses. In contrast to Ca^{2+} responses evoked by the shorter-duration 4- and 5-ns pulses, the Ca^{2+} response of the cells to a 150-ns pulse consisted of a rapid rise in $[Ca^{2+}]_i$ that was mediated not only by Ca^{2+} influx through VGCCs but also as a result of cell membrane permeabilization to Ca^{2+} (23). When the cells were exposed to a 150-ns bipolar pulse, Ca^{2+} influx into the cells was attenuated relative to that evoked by the unipolar pulse. However, only the portion of Ca^{2+} influx attributable to membrane permeabilization was cancelled (24). In other words, the bipolar pulse modulated the Ca^{2+} response of the cells in a way that left the physiological pathway of Ca^{2+} influx through VGCCs unaffected.

In light of these results, this study assessed the existence and parametric limitations of bipolar pulse cancellation of electrostimulation in chromaffin cells exposed to 2-ns pulses, which are closer in duration to those that trigger Ca^{2+} influx solely via VGCCs. We first exposed the cells to a single 2-ns, 16 MV/m unipolar pulse and determined whether Ca^{2+} influx could be cancelled or attenuated with a symmetrical (equal positive and negative phase amplitudes) bipolar pulse. After establishing a cancellation effect, we increased the interval between the two phases of the bipolar pulse from 0 to 120 ns to determine how delivering the second phase of the bipolar pulse after a short delay (tens of nanoseconds) affected the cancellation of Ca^{2+} responses. We also varied the amplitude of the second phase of the bipolar pulse that can affect cancellation efficiency (16). Both manipulations of the bipolar pulse waveform modulated the Ca^{2+} response of the cells and served as a way to test whether the accelerated membrane discharge hypothesis could explain bipolar pulse cancellation in these cells. For the latter, we made a comparison of the experimental results with analytical calculations of the accelerated membrane discharge paradigm and found broad agreement between them. Taken as a whole, the findings of this work have demonstrated that electrostimulation of adrenal chromaffin cells with ultrashort bipolar pulses can modulate Ca^{2+} responses in a manner not previously shown in other cell types and for which insight into a possible underlying mechanism of bipolar cancellation of chromaffin cell electrostimulation has been inferred. Such modulation in an excitable neural-type cell is promising as we work toward the potential use

of synchronized nanosecond bipolar pulse technologies for remote electrostimulation applications.

MATERIALS AND METHODS

Chromaffin cell culturing and preparation

Bovine chromaffin cells were isolated from the medulla of fresh adrenal glands by collagenase digestion and maintained in suspension culture in Ham's F-12 medium supplemented with 10% bovine calf serum, 100 U/mL penicillin, 100 μg/mL streptomycin, 0.25 μg/mL fungizone, and 6 μg/mL cytosine arabinoside at 36.5°C under a humidified atmosphere of 5% CO_2 as previously described (25). Cells were used up until 2 weeks in culture. For all experiments, the large aggregates of cells that form in suspension culture were dissociated into single isolated cells and clusters of two to three cells with the protease dispase (26). Once dissociation was complete, the cells were placed in low-Ca^{2+} balanced salt solution (BSS) with the following composition: 145 mM NaCl, 5 mM KCl, 1.2 mM NaH_2PO_4, 0.5 mM $CaCl_2$, 1.3 mM $MgCl_2$, 10 mM glucose, and 15 mM HEPES (pH 7.4), used to slow the rate of cell reaggregation. Cells were used immediately after dissociation.

Fluorescence imaging of intracellular Ca^{2+}

For Ca^{2+} imaging experiments, cells were incubated with the cell-permeant Ca^{2+} indicator Calcium Green-1 AM (1 μM; $480_{Ex}/535_{Em}$ nm) for 1 h at 37°C in low-Ca^{2+} BSS containing 0.1% bovine serum albumin. After incubation, the cells were centrifuged for 10 min at 30 × g, the supernatant was removed, and the cells were washed twice with dye-free low-Ca^{2+} BSS lacking bovine serum albumin. At the end of the washing steps, the cells were pelleted by centrifugation and resuspended in low-Ca^{2+} BSS. An aliquot of the cell suspension was pipetted into one of the wells of an eight-well glass-bottom chamber (Nunc Lab-Tek II) mounted on the stage of an inverted Leica TCS SP8 laser scanning confocal microscope equipped with a 63× water objective. The chamber well contained BSS (2 mM $CaCl_2$), and the electrodes used for pulse delivery were already immersed in the BSS and positioned for imaging. The cells were allowed to settle between the electrodes (Fig. 1) for 15 min before recording. The final concentration of Ca^{2+} in the well was 1.8 mM.

For experiments conducted in the absence of extracellular Ca^{2+}, 1 mM of the Ca^{2+} chelator EGTA was added to Ca^{2+}-free BSS. For experiments conducted in the absence of extracellular Na^+, an equimolar concentration of N-methyl-D-glucamine ($NMDG^+$) was used to replace Na^+ in the BSS. To block VGCCs, Calcium Green-1-loaded cells were preincubated with 200 μM $CdCl_2$ (Cd^{2+}) in low-Ca^{2+} BSS for 30 min at room temperature before experimentation. Experiments were conducted in BSS containing 1.8 mM $CaCl_2$ and 200 μM Cd^{2+}.

Laser scanning confocal fluorescence microscope images of the cells in suspension were captured every 0.86 s unless otherwise specified. Continuous baseline fluorescence of the cells was monitored 60 s before stimulus application and continued for 6 min after the stimulus. All experiments were performed at ambient room temperature.

Image processing

Cells visible in the microscope field between the electrodes (Fig. 1) were manually selected for fluorescence photometric image analysis before each pulse exposure. Fluorescence intensities of each region of interest were extracted using either custom MATLAB (The MathWorks, Natick, MA) routines or the public domain image processing program ImageJ (https://imagej.nih.gov/ij/). The following built-in MATLAB functions were used in custom image processing routines: "imroi," for manually choosing regions of interest based on transmitted light image membrane boundaries, and "regionprops," for evaluating geometric properties of regions of interest. The change in fluorescence intensity of the cells was calculated by subtracting the cell-free background fluorescence from the fluorescence intensity of the cell ($F = F_{cell}–F_{background}$) and normalized to the intensity value measured when the stimulus was applied (F/F_0).

Pulsed electric field exposure

A FID bipolar pulse generator (FPG 10-1CN6V2; Burbach, Germany) provided 2-ns full width at half maximal Gaussian-shaped unipolar and bipolar electric pulses (Fig. S1 *a*). Pulses were delivered to a group of cells in suspension via a pair of parallel tungsten wire electrodes spaced 70 μm apart (11). Before the experiment, the electrodes were positioned inside the eight-well chamber using a motorized MP-225 micromanipulator (Sutter Instrument, Novato, CA). Unipolar pulses produced an electric field of 16 MV/m (lowest amplitude achievable for a unipolar pulse according to pulse generator specifications) at the location of the cells. The electric field applied was computed by two-dimensional numerical simulations using a finite element analysis software COMSOL Multiphysics (Stockholm, Sweden) as previously reported (11). The electric pulses were monitored using a waveRunner 640Zi digital oscilloscope (Teledyne LeCroy, Chestnut Ridge, NY) at 40 GHz sampling rate. The interval between the two opposite polarity phases (i.e., interphase interval) of the bipolar pulses was varied from no time interval between the end of the first phase and the beginning of the second phase (Fig. S1 *b*) to up to 120 ns, the longest interphase interval achievable on the pulser (Fig. S1, *c–f*). Interphase intervals of 10, 30, 60, and 120 ns were measured from peak/peak for repeatability. Cells were exposed to the electric field either once or multiple times (see Results). The pulse generator is equipped to generate two unipolar pulses of opposite polarity with up to 120-ns separation peak/peak, which can be used to generate bipolar pulses using superposition of the two. By superposition of a larger first phase amplitude and a (device-allowed) minimal amplitude second phase, we were able to adjust the second phase amplitudes with ratios 0.5–2 with respect to the first phase (Fig. S2).

Statistical analysis

Experiments were repeated at least once using cells from different days in culture and different cell preparations. The normalized Ca^{2+} responses of the cells are represented as the mean ± standard error of the mean (SEM). Statistical analysis was done with Microsoft Excel using unpaired Student's *t*-test when the means of two groups were compared. $p < 0.01$ was considered statistically significant.

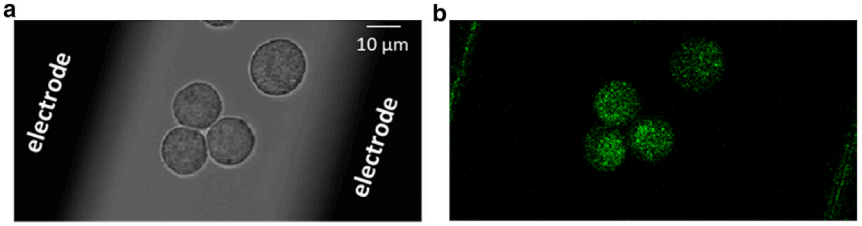

FIGURE 1 Representative bright-field and fluorescence images of chromaffin cells. (*a*) Photomicrograph of cells between the electrodes. (*b*) Fluorescence image of cells loaded with the Ca^{2+} sensitive dye Calcium Green-1. Scale bar, 10 µm. To see this figure in color, go online.

Reagents

Calcium Green-1 AM was purchased from Molecular Probes (Eugene, OR). Ham's F-12 medium and the antibiotic-antimycotic and dispase II were obtained from Gibco Laboratories (Grand Island, NY). Bovine calf serum was purchased from Gemini Bio Products (West Sacramento, CA), and collagenase B was obtained from MilliporeSigma (St. Louis, MO). All other chemicals and reagents were reagent grade and purchased from standard commercial sources.

RESULTS AND DISCUSSION

Exposing chromaffin cells to a single 2-ns, 16 MV/m unipolar pulse evoked a rise in $[Ca^{2+}]_i$ that was abolished by applying a symmetrical 2-ns bipolar pulse

A recent report of chromaffin cell electrostimulation showed that 150-ns unipolar pulses caused Ca^{2+} influx through not only VGCCs but also additional plasma membrane permeabilization. Furthermore, an attenuation (or partial cancellation) of the part of Ca^{2+} influx due to only plasma membrane permeabilization (i.e., excluding VGCC activation) was observed when the cells were exposed to a 150-ns bipolar pulse with equal duration positive and negative phases (24). In our current study, we investigated if the rise in $[Ca^{2+}]_i$ in chromaffin cells elicited by short pulses similar to the 4- and 5-ns pulses used in early experiments, which is the result of VGCC activation (17,18), could be attenuated, cancelled, or otherwise modulated by an electric field reversal applied by bipolar pulses.

Initial experiments established that exposing chromaffin cells to a single 2-ns, 16 MV/m (lowest unipolar pulse amplitude achievable with our exposure setup) unipolar pulse causes similar $[Ca^{2+}]_i$ response characteristics as described for 4- and 5-ns pulses. Fig. 2 *a* shows that the pulse caused an instantaneous, transient rise in $[Ca^{2+}]_i$ (half-width of Ca^{2+} transient ~21 s) that was maximal after 1–2 s (1.63 ± 0.08, $n = 18$ cells) and recovered to baseline within 2–3 min. As previously shown for a 4- or 5-ns pulse, the rise in $[Ca^{2+}]_i$ was abolished in Ca^{2+}-free BSS (Fig. 2 *b*), indicating that the source of Ca^{2+} was extracellular and that there was no Ca^{2+} released as a result of endoplasmic reticulum permeabilization. Preliminary experiments also established that VGCCs mediated the influx of Ca^{2+} because exposing chromaffin cells to the pulse in the presence of Cd^{2+} (200 μM), an inorganic, nonselective blocker of VGCCs (27,28), caused no rise in $[Ca^{2+}]_i$ (Fig. 2 *b*). Fig. 2 *b* shows further that Ca^{2+} influx evoked by a 2-ns pulse, as for a 5-ns pulse, was similarly reliant on external Na^+ because no rise in $[Ca^{2+}]_i$ occurred when cells were exposed in a Na^+-free BSS in which Na^+ was replaced with an equimolar concentration of $NMDG^+$.

Next, to determine if the Ca^{2+} response to this unipolar pulse can be modulated by field reversal, we exposed cells to a 2-ns symmetrical bipolar pulse (equal phase duration and amplitude). Fig. 3 *a* shows that the bipolar pulse did not evoke a rise in $[Ca^{2+}]_i$. In other words, there was a complete cancellation of the response that would have been induced by the first phase of the bipolar pulse alone (Fig. 2 *a*). In addition, cells repeatedly exposed to alternating unipolar and bipolar pulses showed no visible changes in their morphology (Fig. 3 *b*) and no apparent deleterious effects in their response, consistently responding to unipolar exposures at the same level and not responding to bipolar pulse exposures (Fig. 3 *c*). These results indicate that reversing the electric field polarity of an ultrashort, 2-ns pulse is able to cancel Ca^{2+} influx into chromaffin cells in the absence of adverse effects.

Increasing the interval between the phases of the bipolar pulse by only tens of nanoseconds converted cancellation to stimulation

In the next series of experiments, we investigated the effect of increasing the interphase interval on the Ca^{2+} response in chromaffin cells exposed to a 2-ns bipolar pulse. We varied the interphase interval from no delay between the end of the first phase and the beginning of the second phase (i.e., peak/peak measurement of 4 ns) to interphase intervals up to 120 ns (measured peak/peak), keeping the amplitude of the positive and negative phases equal at 16 MV/m. Fig. 4 *c* shows that a 2-ns bipolar pulse with a 10-ns interphase

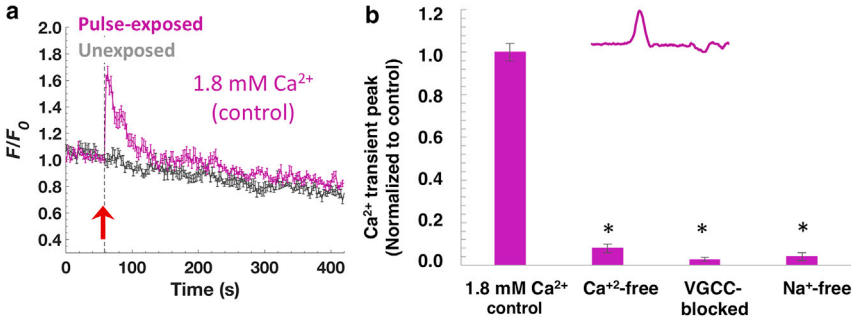

FIGURE 2 Ca^{2+} responses in chromaffin cells exposed to a single 2-ns, 16 MV/m unipolar pulse under different conditions. (*a*) Averaged fluorescence traces ± SEM for unexposed cells (*gray traces*: n = 9) and cells exposed to a 2-ns unipolar pulse (*purple traces*; n = 18). Arrow indicates the time of pulse delivery. (*b*) Comparison of the response of the cells to a 2-ns unipolar pulse in BSS containing 1.8 mM Ca^{2+} (n = 18), in Ca^{2+}-free BSS (n = 5), in BSS with Na^+ replaced with an equimolar concentration of $NMDG^+$ (n = 14), and in BSS containing 1.8 mM Ca^{2+} and 200 μM Cd^{2+} (n = 19). The results are plotted as the mean ± SEM for the Ca^{2+} peaks normalized to the control shown in (*a*). *$p < 0.01$, significantly different from the control. To see this figure in color, go online.

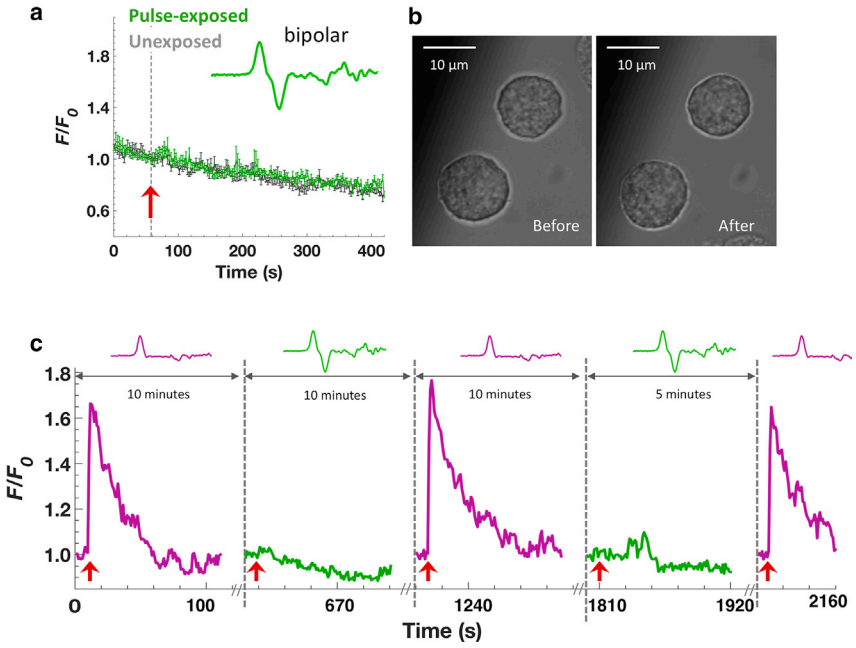

FIGURE 3 Response of chromaffin cells to a 2-ns bipolar pulse. (*a*) Results are plotted as the averaged fluorescence traces ± SEM for unexposed cells (*gray traces*; n = 9) and cells exposed to a symmetrical 2-ns bipolar pulse (*green traces*; n = 9). The arrow indicates the time when the pulse was applied. (*b*) Representative bright-field images of two of the cells before and after exposure to alternating single unipolar and bipolar pulses shown in (*c*). Scale bar, 10 µm. (*c*) Responses of the cells to alternating single 2-ns unipolar and bipolar pulses. Traces represent mean Ca^{2+} responses of 10 cells. Pulse delivery was 10 s into the beginning of each recording indicated by red arrows. To see this figure in color, go online.

interval elicited a Ca^{2+} transient that was reduced significantly in amplitude compared with that elicited by the unipolar pulse (Table 1). Thus, the negative phase of the pulse was already less efficient at cancelling the effect elicited by the positive phase of the pulse. Lengthening the interphase interval to 30 ns elicited Ca^{2+} responses that increased in amplitude to reach a value similar to the one evoked by the unipolar pulse (Fig. 4 *d*). That is, this bipolar pulse waveform was now equivalent to a unipolar pulse with respect to the magnitude of the Ca^{2+} response that was achieved (Table 1). Moreover, as the interphase interval was increased to 60 or 120 ns, Ca^{2+} responses were greater

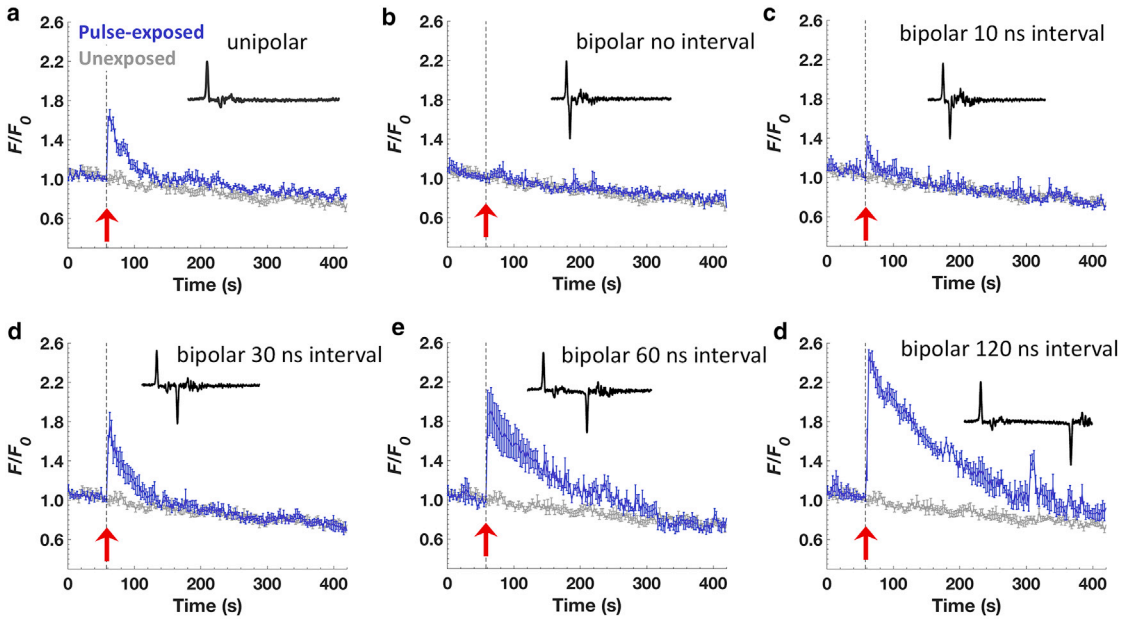

FIGURE 4 Effect of increasing the interphase interval between the positive and negative phase of a 2-ns bipolar pulse on Ca^{2+} responses. (*a*) Response of the cells to a 2-ns unipolar pulse (n = 18). Results are plotted as the averaged fluorescence traces ± SEM for unexposed cells (*gray traces*; n = 9) and pulse-exposed cells (*blue traces*). (*b–f*) Averaged fluorescence traces ± SEM for cells exposed to 2-ns bipolar pulses for interphase intervals of 0 (n = 9), 10 ns (n = 7), 30 ns (n = 8), 60 ns (n = 4), and 120 ns (n = 6), respectively. A representative pulse waveform is provided in each plot, and the arrow indicates the time when the pulse was applied. To see this figure in color, go online.

TABLE 1 Relative $[Ca^{2+}]_i$ Fluorescence Intensity under Different Pulse Exposure Conditions

Pulse Exposure	Mean ± SD	Mean ± SEM	*n* Cells	*t*-Test (*p* Value)
Unipolar	1.68 ± 0.24	1.68 ± 0.04	46	–
Bipolar (no interphase interval)	1.09 ± 0.17	1.09 ± 0.03	25	<0.01
Bipolar (10-ns interval)	1.29 ± 0.22	1.29 ± 0.05	21	<0.01
Bipolar (30-ns interval)	1.77 ± 0.30	1.77 ± 0.07	16	0.26
Bipolar (60-ns interval)	2.19 ± 0.34	2.19 ± 0.08	18	<0.01
Bipolar (120-ns interval)	2.54 ± 0.11	2.54 ± 0.05	6	<0.01

An unpaired Student's *t*-test was used to compare the peaks of each bipolar exposure to that of the unipolar exposure.

in magnitude than those evoked by the unipolar pulse (Fig. 4, *e* and *f*; Table 1), which we call stimulation. The mean Ca^{2+} traces with different interphase interval exposures are plotted together in Fig. 5 *a*, and the averaged peak values ± SEM with respect to that of unipolar exposures are summarized in Fig. 5 *b*. Taken as a whole, these results indicate that the interphase interval of a 2-ns bipolar pulse is not only critical for modulating chromaffin cell excitability but that the transition between cancellation and stimulation that can be achieved occurs with interphase intervals on the order of tens of nanoseconds.

Varying the amplitude of the negative phase of the 2-ns bipolar pulse also modulated $[Ca^{2+}]_i$

The results presented in Figs. 4 and 5 obtained by varying the interphase interval of the bipolar pulse are the first observations of a biological response being modulated within such a short window of time, tens of nanoseconds, between the two phases of the bipolar pulse. Because chromaffin cells (~16 μm in diameter (29)) have a membrane-charging time constant (τ_m) around 100 ns (30), these results are consistent with the possibility that the accelerated (assisted) membrane discharge mechanism (10) is playing a role in these observations. As discussed earlier, accelerated membrane discharge comes from a simple capacitive electrical model of the cell membrane that is charged during the first positive phase of a bipolar pulse and the discharge is accelerated because of the second negative phase, thereby reducing the time over which the membrane potential is above a critical potential. This mechanism, which was previously discussed in detail in Sözer and Vernier (11) and further addressed in relation to these results in the following section, suggests that the cancellation should be a function of not only the timing of the second phase but also its relative amplitude with respect to the first phase (11).

To test this mechanistic hypothesis, we varied the second phase amplitude ratio (ratio of the amplitude of the second phase to that of the first phase) from 0.5 to 2 for a bipolar pulse with no interphase interval, keeping the positive phase in all cases set to 16 MV/m. As shown in Fig. 6, we found that the rise in $[Ca^{2+}]_i$ was still cancelled even when the amplitude of the second phase was only half that of the first phase. Increasing the second phase amplitude ratios to values that ranged from 1.5 to 1.8 caused a progressive loss of cancellation. At a second phase amplitude ratio of 2, there was no longer cancellation but instead stimulation (relative to the equivalent unipolar pulse). The mean Ca^{2+} traces with different second phase amplitude exposures are plotted together in Fig. 7 *a*, and the averaged peak values ± SEM with respect to that of unipolar exposure are summarized in Fig. 7 *b*. These results indicate that modulation of chromaffin cell electrostimulation by 2-ns bipolar pulses, going from complete cancellation to stimulation beyond the unipolar-equivalent level, is sensitive not only to very short, tens of nanoseconds intervals between the two phases but also to the relative amplitude of the second phase to that of the first, showing a gradual transition of the Ca^{2+} response within the second phase ratio range of 0.5–2.

The experimental results obtained for both manipulations of the bipolar pulse waveform are consistent with the accelerated membrane discharge hypothesis

One of the first hypotheses proposed to explain the process of attenuation or "cancellation" of biological effects by electric field reversal was the accelerated (or assisted) membrane

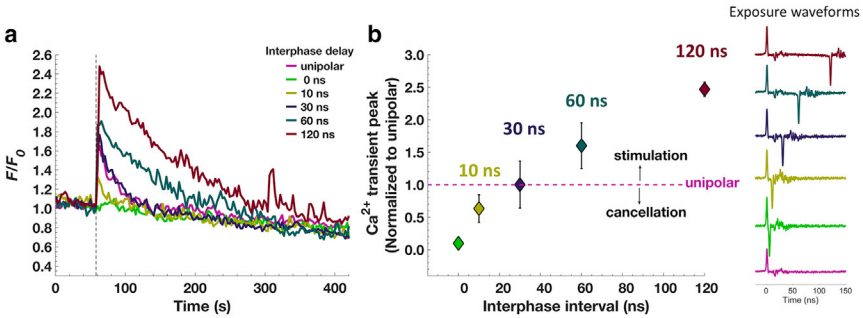

FIGURE 5 Cancellation versus stimulation of Ca^{2+} responses for different interphase intervals of a 2-ns bipolar pulse. (*a*) Results are plotted as the averaged fluorescence traces for cells exposed to a 2-ns unipolar pulse or a 2-ns bipolar pulse with various interphase delays (data from different panels of Fig. 4). (*b*) Peak amplitudes of Ca^{2+} transients with respect to unipolar exposure peak ± SEM (n = 18 for the unipolar pulse, n = 9, 7, 8, 4, and 6 cells for bipolar pulses with 0-, 10-, 30-, 60-, and 120-ns interphase intervals, respectively). Cumulative results including additional experiments are summarized in Table 1 and provided in Fig. S3. To see this figure in color, go online.

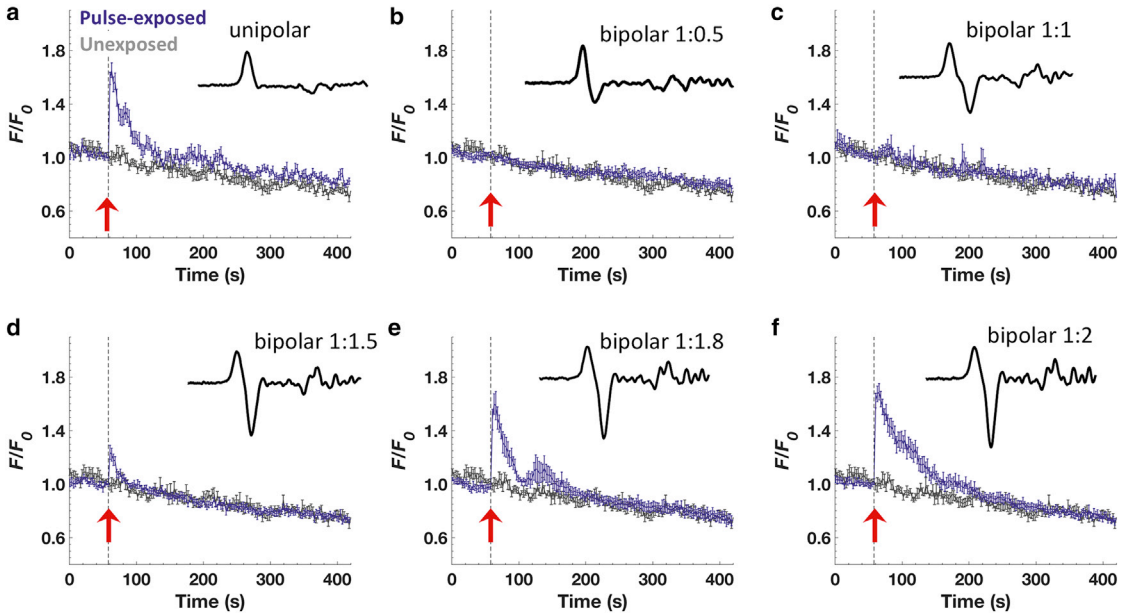

FIGURE 6 Effect of varying the amplitude of the second phase of the 2-ns bipolar pulse on Ca^{2+} responses. (*a*) Response of the cells to a 2-ns unipolar pulse (n = 18). Results are plotted as the averaged fluorescence traces ± SEM for unexposed cells (*gray traces*; n = 9) and pulse-exposed cells (*blue traces*). (*b–f*) Averaged fluorescence traces ± SEM for cells exposed to 2-ns bipolar pulses for second phase amplitude ratios of 0.5 (n = 16), 1.0 (n = 9), 1.5 (n = 23), 1.8 (n = 8), and 2.0 (n = 24), respectively. A representative pulse waveform is provided in each plot, and the arrow indicates the time when the pulse was applied. To see this figure in color, go online.

discharge hypothesis (10,15). Accelerated discharge mechanism assumes that the cell membrane is a nonconductive dielectric shell that electrically behaves as a resistor-capacitor circuit with a charging time constant τ_m = resistor-capacitor. In this simplified cell membrane model, the time-dependent membrane potential, $V_m(t)$, under the influence of an external field can be calculated as follows:

$$V_m(t) = V_{m,0} + (V_{m,induced} - V_{m,0})\left(1 - \exp\left(-\frac{t - t_0}{\tau_m}\right)\right), \quad (1)$$

where $V_{m,0}$ is the initial membrane potential at time t_0, $V_{m,induced}$ is the induced potential by the external electric field, and τ_m is the membrane-charging time constant, which is a function of intracellular and extracellular conductivities and cell size (30).

Calculations based on this hypothesis show that the effect of charging during the first phase of the bipolar pulse can be flexibly modulated by the second phase, depending on two parameters, as follows: 1) its timing, which affects t_0 in Eq. 1, and 2) its amplitude, which affects the amplitude of $V_{m,induced}$ in Eq. 1 (11). Moreover, the modulation of cancellation by changing t_0 and $V_{m,induced}$ would be more sensitive to these parameters as the pulse duration approaches the membrane-charging time constant, τ_m (~100 ns). This implies a very restricted parameter range in which an attenuation compared with the unipolar-evoked response is observed. This sensitivity and consequential restriction in

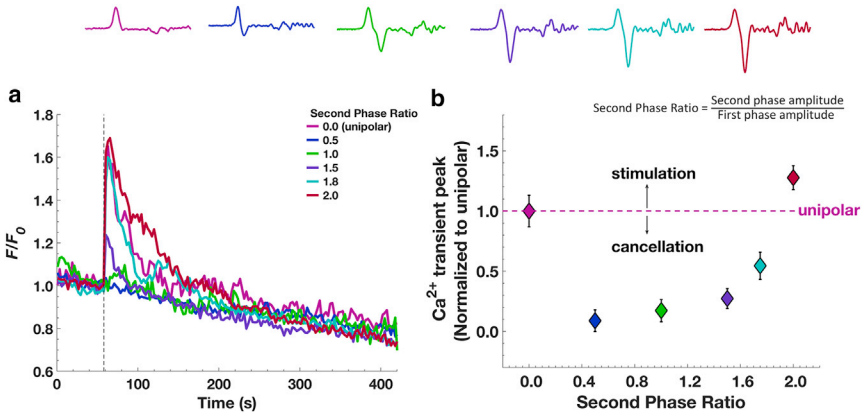

FIGURE 7 Cancellation versus stimulation of Ca^{2+} responses for different amplitudes of the second phase of a 2-ns bipolar pulse. (*a*) Results are plotted as the averaged fluorescence traces for cells exposed to a 2-ns unipolar pulse or a 2-ns bipolar pulse for second phase amplitude ratios varying from 0.0 (unipolar) to 2. (*b*) Results are peak amplitudes of Ca^{2+} transients ± SEM (n = 18, 16, 9, 23, 8, and 24 for second phase amplitude ratios of 0.0, 0.5, 1.0, 1.5, 1.8, and 2, respectively). To see this figure in color, go online.

parameter ranges for observing different phases of modulation, in theory, should be easily demonstrated as the cancellation (or attenuation) transitions to amplification approaching to the effect of two unipolar pulses. Interestingly, with a bipolar pulse, an amplification approaching to the effect of two unipolar pulses was not reported in any prior reports with pulse durations ranging from 2 to 900 ns (11). Moreover, earlier experimental results using pulse durations in the order of the membrane-charging time constant τ_m (~100 ns) have shown that interphase intervals as high as 50 μs still resulted in bipolar cancellation (10,15), which cannot be explained with this hypothesis.

In our current study, we used 2-ns pulses, which are significantly shorter than the membrane-charging time constant (τ_m) of typical mammalian cells, including chromaffin cells. The short duration of the pulse allows a linear approximation of the exponential in Eq. 1 and makes the predictions of calculations of accelerated discharge simpler and less sensitive to statistical variations in experimental conditions. Equation 1 predicts a minimal response with equal negative and positive phase amplitudes for a large range of values of membrane-charging time constant, τ_m, if it is significantly longer than 2 ns. The, to our knowledge, novel observation in our experiments, which is the time frame for modulation of electrostimulation being tens of nanoseconds, is consistent with the accelerated membrane discharge hypothesis, unlike any of the prior investigations.

Therefore, we repeated our previous calculations (11) for the accelerated membrane discharge for chromaffin cells and varied the interphase intervals to evaluate the degree of consistency between this analytical model and our experimental results. Fig. 8, *a–c* shows the calculated maximal membrane potential kinetics for varying interphase delays. As a metric of effectiveness of each pulse exposure, we used the integrated product of membrane potential above a certain threshold (0.5 V for these calculations) and time, A_{eff}. We chose 0.5 V as a midrange among the values used in the literature for the electropermeabilization threshold of membranes (31–37). Although the induced potential will vary depending on the location on the membrane with respect to the direction of the electric field (30), it stays above 0.5 V except for a 20° slice around the equator of the cell, meaning that most of the cell surface is exposed to an induced potential higher than this threshold. This high induced potential is also not significantly modified by the resting potential of chromaffin cells, which is reported to be in the range of −40 to −80 mV (38,39).

Fig. 8 *d* shows the predicted effectiveness normalized to that of unipolar pulse exposure together with the normalized peak amplitudes of the $[Ca^{2+}]_i$ transients to that of a unipolar

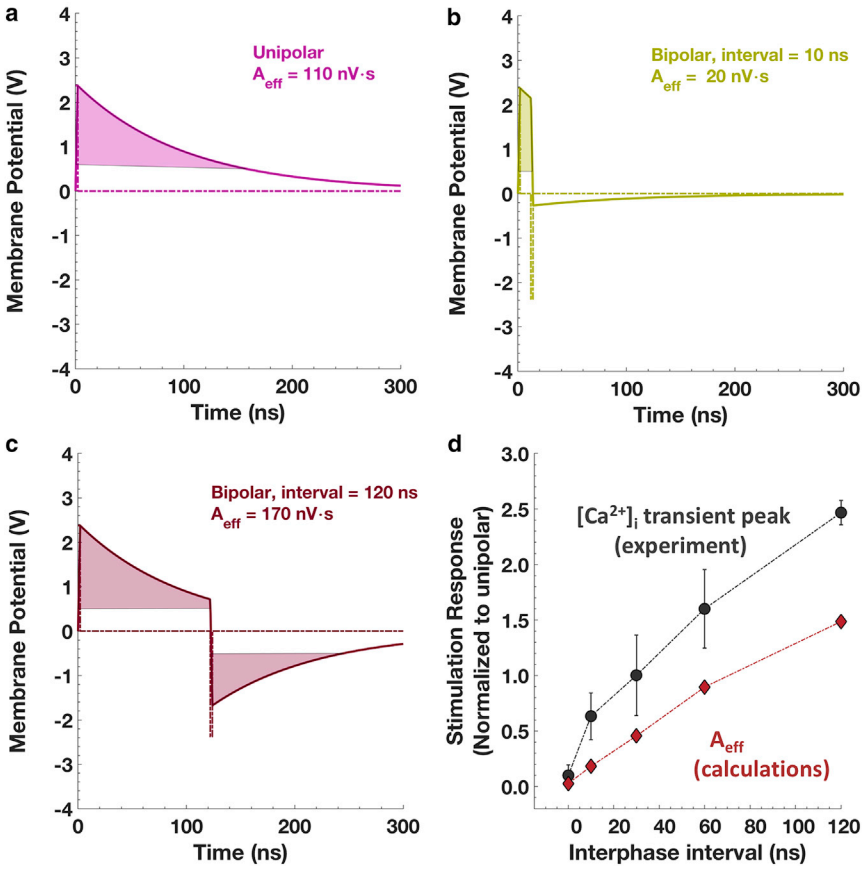

FIGURE 8 Accelerated membrane discharge calculations of 2-ns, 16 MV/m pulses. (*a*) Unipolar pulse, (*b*) bipolar pulse with 10-ns interphase interval, and (*c*) bipolar pulse with 120-ns interphase interval. (*d*) Comparison of calculated and experimental effectiveness of bipolar pulses with changing interphase intervals with respect to unipolar pulse exposure. The error bars represent the SEM. To see this figure in color, go online.

pulse measured in experiments (Figs. 4 and 5). We observe a rate of increase of normalized effectiveness that matches the experiments, whereas the normalized absolute values surpass the prediction by around 60% (Fig. 8 *d*) at each point.

The simple capacitive membrane model in the accelerated discharge hypothesis assumes that even after a very high membrane potential is induced across the membrane, the permeabilization and subsequent change in membrane conductivity are not substantial enough to cause a drop in the membrane potential. This is contradictory to the pore evolution modeled in standard electroporation models, in which the postpulse membrane potential goes quickly to 0 because of the change in membrane conductivity (40–42). In other words, if the membrane conductivity increases significantly during the first phase of a bipolar pulse exposure, the resulting permeant membrane can no longer maintain a potential difference. In this case, a following pulse of opposite polarity cannot discharge (or charge) the membrane, and "cancellation" is impossible. Indeed, for pure lipid systems, we have shown that immediately after, the second pulse of opposite polarity does not affect transport through the lipid bilayer and thus does not cause a "cancellation" effect (43).

Another way to test the unaltered postpulse membrane potential assumption is by varying the amplitude of the second phase without any interphase interval. Experimental results for several cases (Figs. 6 and 7) show that the pulse-stimulated increase of intracellular Ca^{2+} in chromaffin cells is highly dependent on the amplitude of the second phase of the bipolar pulse. Thus, the membrane is not likely to be highly conductive, as it is represented in classical continuum electroporation models. Theoretical results for several cases are shown in Fig. 9, *a–c*. Fig. 9 *d* shows the calculated (based on A_{eff}) and experimental (based on the peak amplitude of the $[Ca^{2+}]_i$ transient) effectiveness with respect to the unipolar pulse, which are in good agreement. This suggests that the mechanism of activation likely involves membrane charging and is not complicated by voltage-gated responses of ion channels as with traditional neuronal stimulation thresholds (44–46). As we know from our earlier work (19) and our data with a unipolar pulse (Fig. 2 *b*), the mechanism involves permeabilization to Na^+ to a level that is sufficient to activate VGCCs. This permeabilization, however, does not appear to affect the conductivity of the membrane enough to cause a drop in postpulse potential as predicted by electroporation models (42), which would eliminate the transmembrane potential that would be discharged by a following pulse of opposite polarity. In contrast, for longer duration pulses such as the 150-ns pulses used in our previous study (24), the membrane appeared to be permeable also to Ca^{2+}, and in that case, postpulse membrane potential may have been significantly altered. Thus,

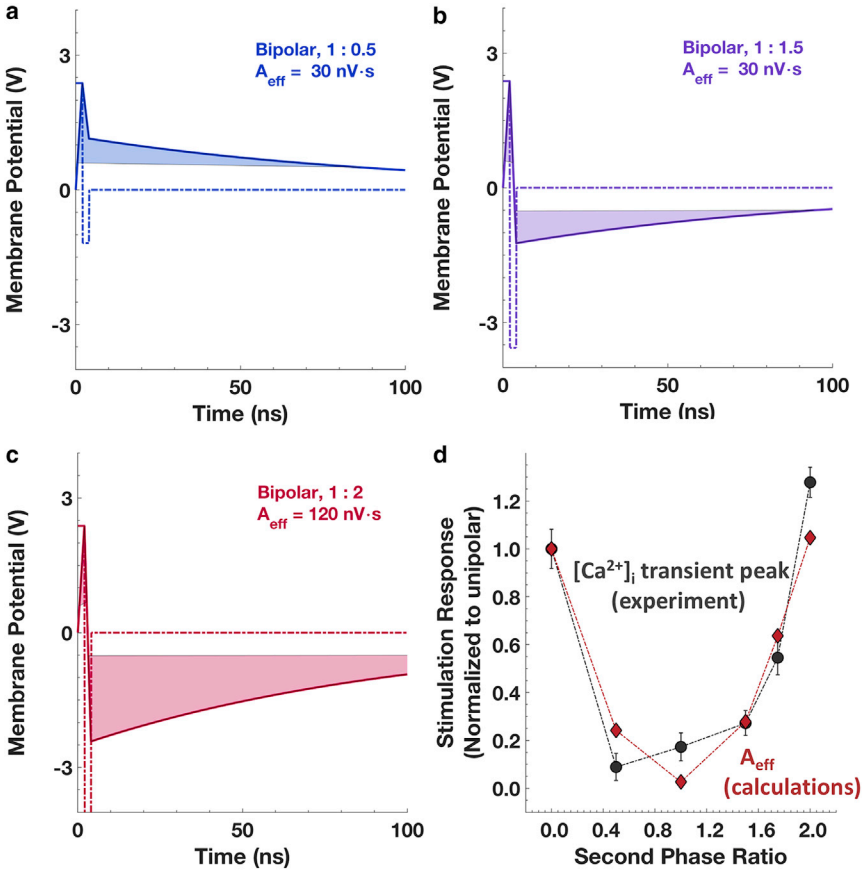

FIGURE 9 Accelerated membrane discharge calculations of 2-ns, 16 MV/m bipolar pulse with various second phase ratios. (*a*) Second phase ratio of 0.5, (*b*) 1.5, and (*c*) 2. (*d*) Comparison of calculated and experimental effectiveness of bipolar pulses with changing second phase ratio with respect to unipolar pulse exposure. The error bars represent the SEM. To see this figure in color, go online.

the accelerated discharge hypothesis as presented here would not be sufficient to model the complex events that result in Ca^{2+} influx into cells through multiple pathways.

These electrostimulation results in chromaffin cells showing consistency with the accelerated membrane discharge hypothesis contrast with previous results obtained from electropermeabilization experiments, which could not be explained by this hypothesis (10,11,15,16). A possible interpretation pertains to a very important difference between the experimental conditions used here versus those used in the other studies, the dose of the pulsed electric field. The single 16 MV/m nanosecond pulse used to electrostimulate chromaffin cells was significantly smaller than earlier studies with much longer pulses or much higher field and pulse numbers. Note that the high electric field amplitudes required for electropermeabilization mean significantly higher effective areas (A_{eff}) in our theoretical calculations based on the simple model of membranes represented as perfect capacitors. The higher dose is also more likely to modify the electrical properties of the cell membrane so much that the accelerated discharge analysis no longer applies. Under these conditions, we are more likely to observe the results of a multistep process, which includes complex biological responses to the initial impact of the membrane charging. In other words, the accelerated membrane discharge mechanism describes the functional behavior of adrenal chromaffin cells in the low-dose, electrostimulation regime but may not be adequate for higher-dose, electropermeabilization conditions.

CONCLUSIONS

This study shows that the rapid, transient influx of Ca^{2+} via VGCCs that is evoked in isolated neuroendocrine adrenal chromaffin cells by a single unipolar 2-ns pulse can be abolished or attenuated by immediately delivering a second pulse having the same duration and amplitude but opposite polarity. In our previous studies in which chromaffin cells were stimulated with a single 150-ns pulse, cancellation of Ca^{2+} influx via VGCCs was not achieved by an electric field reversal (24), demonstrating that in these excitable cells, the duration of the pulse used for electrostimulation is critical for a cancelling effect of this response by bipolar pulses.

The novel feature of the electrostimulation modality described here is that depending on the interphase interval of the bipolar pulse, Ca^{2+} responses are modulated within a very short temporal scale, on the order of tens of nanoseconds. Specifically, only a 30-ns separation between the positive and negative phases of a 2-ns bipolar pulse is enough to go from cancellation to unipolar-equivalent responses in chromaffin cells without any deleterious effects to the cells. In other studies in which the attenuation or cancellation of various effects of electric pulse exposures using different bipolar pulse waveforms have been explored, the recovery of unipolar-equivalent responses took microseconds, sometimes up to 50 μs between the two phases of the bipolar pulses (8–10,12). When viewing this difference of a nanosecond versus a microsecond interphase interval from a practical standpoint, one consideration is that for remote stimulation capabilities, shorter pulse durations and interphase intervals not only lead to higher capacity of modulation because of the higher frequency content of the pulses (14) but also enable remote targeting over longer distances. The latter is because a short-duration unipolar pulse, even when attenuated over a long distance, can result in a more effective exposure than the one caused by a higher-amplitude bipolar pulse with an effective exposure area near the electrostimulation source (7). Another consideration is that for neuromodulation, nanosecond bipolar pulses having interphase intervals of only nanoseconds expose cells/tissues to a shorter-duration bipolar pulse, which also increases the likelihood of damage-free recovery.

Establishing that our experimental results show consistency with a proposed mechanism of bipolar pulse cancellation, the accelerated membrane discharge hypothesis, is important for future efforts aimed at developing nanosecond bipolar pulse technologies for neuromodulation. Important to note, however, is that unlike other studies that examined cancellation of a primary effect of nanosecond pulse exposure, plasma membrane electropermeabilization, Ca^{2+} influx via VGCCs is a downstream effect. Moreover, although the cellular basis underlying VGCC activation by ultrashort nanosecond pulses is consistent with a reversible permeabilization of the plasma membrane to Na^+ that leads to membrane depolarization sufficient in magnitude to activate VGCCs (19,22), the nature of the pathway of Na^+ influx, electropermeabilization of the lipid bilayer, and/or Na^+ influx via a nonselective cation channel (19) is not yet established. Thus, the primary cellular response that is cancelled remains to be determined and will be the subject of future studies.

SUPPORTING MATERIAL

Supporting Material can be found online at https://doi.org/10.1016/j.bpj.2020.12.017.

AUTHOR CONTRIBUTIONS

J.Z., E.B.S., G.L.C., and P.T.V. planned the research. E.B.S. and J.Z. designed and performed the experiments and analyzed the experimental data. E.B.S. performed the theoretical calculations and analysis and built custom scripts for experimental and theoretical data plots. J.Z. and E.B.S. wrote the manuscript. G.L.C. wrote part of the manuscript and edited and revised the whole manuscript. N.L. and P.T.V. revised the manuscript and contributed to discussions. G.L.C. provided adrenal chromaffin cells. All experiments were performed in P.T.V.'s laboratory.

ACKNOWLEDGMENTS

The authors thank Drs. Lisha Yang and Tarique Bagalkot for chromaffin cell preparation help, Rita Aoun and Kyle Murray for technical help, and Wolf

Pack Meats, University of Nevada, Reno for providing fresh bovine adrenal glands.

This work was supported by AFOSR MURI grant (FA9550-15-1-0517) and in part by AFOSR grants (FA9550-14-1-0018) and (FA9550-14-1-0123).

REFERENCES

1. Volkmann, J., J. Herzog, …, G. Deuschl. 2002. Introduction to the programming of deep brain stimulators. *Mov. Disord.* 17 (*Suppl 3*):S181–S187.
2. Mayberg, H. S., A. M. Lozano, …, S. H. Kennedy. 2005. Deep brain stimulation for treatment-resistant depression. *Neuron.* 45:651–660.
3. Deng, Z. D., S. H. Lisanby, and A. V. Peterchev. 2013. Electric field depth-focality tradeoff in transcranial magnetic stimulation: simulation comparison of 50 coil designs. *Brain Stimul.* 6:1–13.
4. Ji, R. R., T. E. Schlaepfer, …, F. Rupp. 1998. Repetitive transcranial magnetic stimulation activates specific regions in rat brain. *Proc. Natl. Acad. Sci. USA.* 95:15635–15640.
5. Jiang, N., and B. Y. Cooper. 2011. Frequency-dependent interaction of ultrashort E-fields with nociceptor membranes and proteins. *Bioelectromagnetics.* 32:148–163.
6. Casciola, M., S. Xiao, and A. G. Pakhomov. 2017. Damage-free peripheral nerve stimulation by 12-ns pulsed electric field. *Sci. Rep.* 7:10453.
7. Gianulis, E. C., M. Casciola, …, A. G. Pakhomov. 2019. Selective distant electrostimulation by synchronized bipolar nanosecond pulses. *Sci. Rep.* 9:13116.
8. Casciola, M., S. Xiao, …, A. G. Pakhomov. 2019. Cancellation of nerve excitation by the reversal of nanosecond stimulus polarity and its relevance to the gating time of sodium channels. *Cell. Mol. Life Sci.* 76:4539–4550.
9. Ibey, B. L., J. C. Ullery, …, A. G. Pakhomov. 2014. Bipolar nanosecond electric pulses are less efficient at electropermeabilization and killing cells than monopolar pulses. *Biochem. Biophys. Res. Commun.* 443:568–573.
10. Pakhomov, A. G., I. Semenov, …, B. L. Ibey. 2014. Cancellation of cellular responses to nanoelectroporation by reversing the stimulus polarity. *Cell. Mol. Life Sci.* 71:4431–4441.
11. Sözer, E. B., and P. T. Vernier. 2019. Modulation of biological responses to 2 ns electrical stimuli by field reversal. *Biochim. Biophys. Acta Biomembr.* 1861:1228–1239.
12. Gianulis, E. C., J. Lee, …, A. G. Pakhomov. 2015. Electroporation of mammalian cells by nanosecond electric field oscillations and its inhibition by the electric field reversal. *Sci. Rep.* 5:13818.
13. Valdez, C. M., R. A. Barnes, Jr., …, B. L. Ibey. 2017. Asymmetrical bipolar nanosecond electric pulse widths modify bipolar cancellation. *Sci. Rep.* 7:16372.
14. Merla, C., A. G. Pakhomov, …, P. T. Vernier. 2017. Frequency spectrum of induced transmembrane potential and permeabilization efficacy of bipolar electric pulses. *Biochim. Biophys. Acta Biomembr.* 1859:1282–1290.
15. Gianulis, E. C., M. Casciola, …, A. G. Pakhomov. 2018. Electropermeabilization by uni- or bipolar nanosecond electric pulses: the impact of extracellular conductivity. *Bioelectrochemistry.* 119:10–19.
16. Pakhomov, A. G., S. Grigoryev, …, S. Xiao. 2018. The second phase of bipolar, nanosecond-range electric pulses determines the electroporation efficiency. *Bioelectrochemistry.* 122:123–133.
17. Vernier, P. T., Y. Sun, …, G. L. Craviso. 2008. Nanosecond electric pulse-induced calcium entry into chromaffin cells. *Bioelectrochemistry.* 73:1–4.
18. Craviso, G. L., P. Chatterjee, …, P. T. Vernier. 2009. Nanosecond electric pulse-induced increase in intracellular calcium in adrenal chromaffin cells triggers calcium-dependent catecholamine release. *IEEE Trans. Dielectr. Electr. Insul.* 16:1294–1301.
19. Craviso, G. L., S. Choe, …, P. T. Vernier. 2010. Nanosecond electric pulses: a novel stimulus for triggering Ca^{2+} influx into chromaffin cells via voltage-gated Ca^{2+} channels. *Cell. Mol. Neurobiol.* 30:1259–1265.
20. Craviso, G. L., S. Choe, …, P. T. Vernier. 2012. Modulation of intracellular Ca^{2+} levels in chromaffin cells by nanoelectropulses. *Bioelectrochemistry.* 87:244–252.
21. Bornstein, S. R., M. Ehrhart-Bornstein, …, R. Levi-Montalcini. 2012. Chromaffin cells: the peripheral brain. *Mol. Psychiatry.* 17:354–358.
22. Yoon, J., N. Leblanc, …, G. L. Craviso. 2016. Enhanced monitoring of nanosecond electric pulse-evoked membrane conductance changes in whole-cell patch clamp experiments. *J. Membr. Biol.* 249:633–644.
23. Bagalkot, T. R., R. C. Terhune, …, G. L. Craviso. 2018. Different membrane pathways mediate Ca^{2+} influx in adrenal chromaffin cells exposed to 150–400 ns electric pulses. *BioMed Res. Int.* 2018:9046891.
24. Bagalkot, T. R., N. Leblanc, and G. L. Craviso. 2019. Stimulation or cancellation of Ca^{2+} influx by bipolar nanosecond pulsed electric fields in adrenal chromaffin cells can be achieved by tuning pulse waveform. *Sci. Rep.* 9:11545.
25. Hassan, N., I. Chatterjee, …, G. L. Craviso. 2002. Mapping membrane-potential perturbations of chromaffin cells exposed to electric fields. *IEEE Trans. Plasma Sci.* 30:1516–1524.
26. Craviso, G. L. 2004. Generation of functionally competent single bovine adrenal chromaffin cells from cell aggregates using the neutral protease dispase. *J. Neurosci. Methods.* 137:275–281.
27. Weinsberg, F., U. Bickmeyer, and H. Wiegand. 1995. Effects of inorganic mercury (Hg^{2+}) on calcium channel currents and catecholamine release from bovine chromaffin cells. *Arch. Toxicol.* 69:191–196.
28. Owen, P. J., R. Plevin, and M. R. Boarder. 1989. Characterization of bradykinin-stimulated release of noradrenaline from cultured bovine adrenal chromaffin cells. *J. Pharmacol. Exp. Ther.* 248:1231–1236.
29. Zaklit, J., G. L. Craviso, …, I. Chatterjee. 2017. Adrenal chromaffin cells exposed to 5-ns pulses require higher electric fields to porate intracellular membranes than the plasma membrane: an experimental and modeling study. *J. Membr. Biol.* 250:535–552.
30. Kotnik, T., G. Pucihar, and D. Miklavčič. 2010. Induced transmembrane voltage and its correlation with electroporation-mediated molecular transport. *J. Membr. Biol.* 236:3–13.
31. Benz, R., F. Beckers, and U. Zimmermann. 1979. Reversible electrical breakdown of lipid bilayer membranes: a charge-pulse relaxation study. *J. Membr. Biol.* 48:181–204.
32. Kinosita, K., Jr., and T. Y. Tsong. 1977. Voltage-induced pore formation and hemolysis of human erythrocytes. *Biochim. Biophys. Acta.* 471:227–242.
33. Teissie, J., and T. Y. Tsong. 1981. Electric field induced transient pores in phospholipid bilayer vesicles. *Biochemistry.* 20:1548–1554.
34. Robello, M., and A. Gliozzi. 1989. Conductance transition induced by an electric field in lipid bilayers. *Biochim. Biophys. Acta.* 982:173–176.
35. Chernomordik, L. V., S. I. Sukharev, …, Y. A. Chizmadzhev. 1987. The electrical breakdown of cell and lipid membranes: the similarity of phenomenologies. *Biochim. Biophys. Acta.* 902:360–373.
36. Marszalek, P., D. S. Liu, and T. Y. Tsong. 1990. Schwan equation and transmembrane potential induced by alternating electric field. *Biophys. J.* 58:1053–1058.
37. Teissié, J., and M. P. Rols. 1993. An experimental evaluation of the critical potential difference inducing cell membrane electropermeabilization. *Biophys. J.* 65:409–413.
38. Lingle, C. J., P. L. Martinez-Espinosa, …, E. Carbone. 2018. Roles of Na^{+}, Ca^{2+}, and K^{+} channels in the generation of repetitive firing and rhythmic bursting in adrenal chromaffin cells. *Pflugers Arch.* 470:39–52.
39. Fenwick, E. M., A. Marty, and E. Neher. 1982. A patch-clamp study of bovine chromaffin cells and of their sensitivity to acetylcholine. *J. Physiol.* 331:577–597.
40. DeBruin, K. A., and W. Krassowska. 1999. Modeling electroporation in a single cell. I. Effects of field strength and rest potential. *Biophys. J.* 77:1213–1224.

41. Gowrishankar, T. R., K. C. Smith, and J. C. Weaver. 2013. Transport-based biophysical system models of cells for quantitatively describing responses to electric fields. *Proc. IEEE.* 101:505–517.

42. Son, R. S., K. C. Smith, …, J. C. Weaver. 2014. Basic features of a cell electroporation model: illustrative behavior for two very different pulses. *J. Membr. Biol.* 247:1209–1228.

43. Sözer, E. B., S. Haldar, …, J. Zimmerberg. 2020. Dye transport through bilayers agrees with lipid electropore molecular dynamics. *Biophys. J.* 119:1724–1734.

44. Wang, B., A. S. Aberra, …, A. V. Peterchev. 2018. Modified cable equation incorporating transverse polarization of neuronal membranes for accurate coupling of electric fields. *J. Neural Eng.* 15:026003.

45. Krassowska, W., and J. C. Neu. 1994. Response of a single cell to an external electric field. *Biophys. J.* 66:1768–1776.

46. Boinagrov, D., J. Loudin, and D. Palanker. 2010. Strength-duration relationship for extracellular neural stimulation: numerical and analytical models. *J. Neurophysiol.* 104:2236–2248.

Biophysical Journal, Volume *120*

Supplemental Information

2-ns Electrostimulation of Ca^{2+} Influx into Chromaffin Cells: Rapid Modulation by Field Reversal

Josette Zaklit, Gale L. Craviso, Normand Leblanc, P. Thomas Vernier, and Esin B. Sözer

Pulse exposure waveforms

A 2 ns bipolar pulse generator (FID GmbH FPG 10-1CN6V2, Burbach, Germany) was used to deliver unipolar and bipolar electric pulses. Pulse traces were captured during each experiment using a waveRunner 640Zi digital oscilloscope (Teledyne LeCroy, Chestnut Ridge, NY). The interphase interval of the bipolar pulses was varied from no time interval between the end of the first phase and the beginning of the second phase to up to 120 ns (longest interphase interval achievable on the pulser) (Figure S1). Interphase intervals of 10, 30, 60 and 120 ns were measured from peak-to-peak for repeatability.

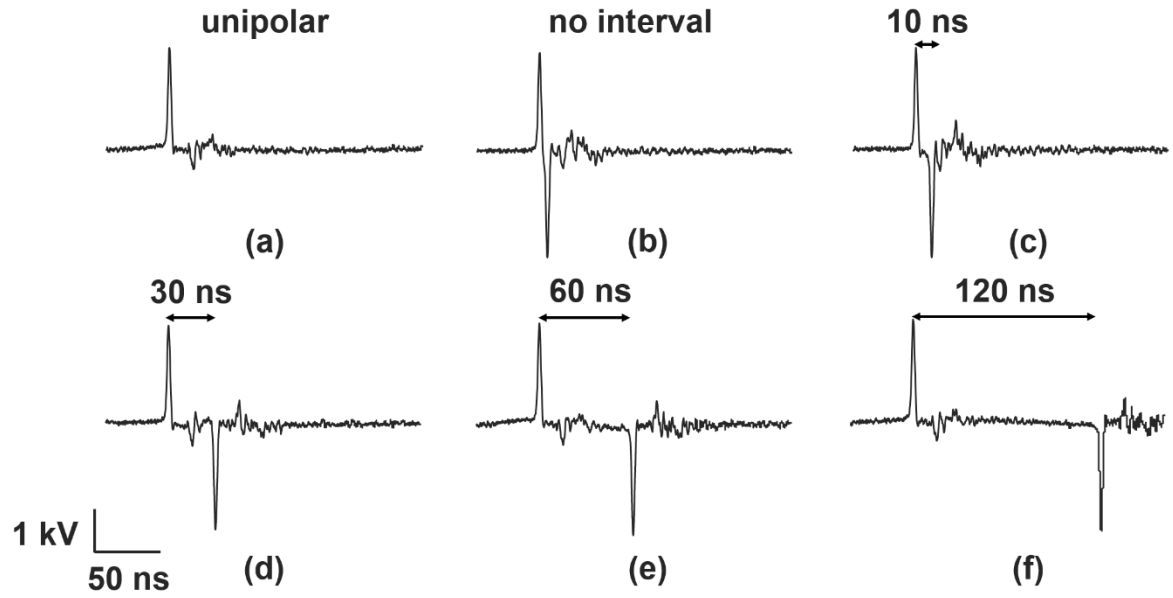

FIGURE S1 Representative oscilloscope traces of 2 ns unipolar and bipolar pulses having the same positive and negative phases but varying the interphase interval. (a) Unipolar pulse, (b) Bipolar pulse with no interphase interval, and (c) to (f) bipolar pulses with interphase intervals ranging from 10 to 120 ns, respectively, measured from peak to peak. In all plots, the amplitudes of the positive and negative phase are equal to ±1.8 kV. There is a small reflection of the pulse at the load so we accounted for that in the field calculation at the cells, which comes to the peak potential difference for the cells to see ~1.5 kV.

For experiments where the amplitude of the second (negative) phase of the bipolar pulse was changed, the second phase amplitude ratio was changed from 0.5:2 by superposition of a larger first phase amplitude and a (device-allowed) minimum amplitude second phase (Figure S2).

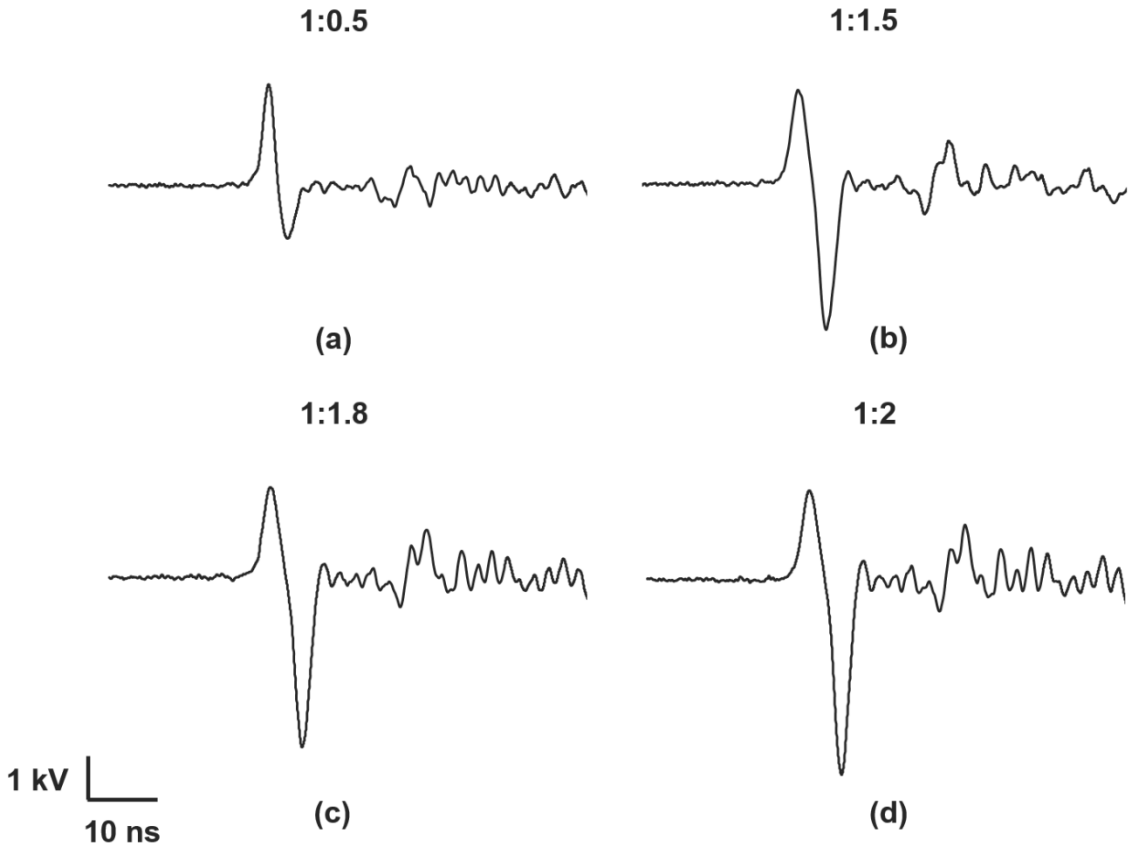

FIGURE S2 Representative oscilloscope traces of 2 ns unipolar and bipolar pulses with no interphase interval obtained by varying the amplitude of the second phase. (a) to (d) Bipolar pulses in which the positive phase was set to +1.8 kV and the negative pulse phase varied in amplitude from 0.9 kV to 3.6 kV, respectively. The second phase amplitude ratios (ratio of the amplitude of the second phase to that of the first phase) are indicated in each plot and varied from 0.5 to 2. The reflections were accounted for in the field calculations assuming the same amount as in the unipolar pulse.

Time course of the mean response of cells to unipolar and bipolar exposures with varying interphase intervals (cumulative results)

For experiments in which we varied the interphase interval from no delay between the positive and negative phase of the bipolar pulse to up to 120 ns, Figure S3 shows the cumulative results obtained from this study. These results represent the total number of cells exposed to the various pulses. Results shown in Figure 4 of the manuscript represent only a few number of cells tested. Continuous baseline fluorescence of the cells was monitored 60 s prior to stimulus application and continued for up to 5 min after the stimulus. Responses were monitored up until they returned to baseline.

The results showed that a 2 ns bipolar pulse with no interphase interval completely cancels the response elicited by the unipolar pulse. A 10 ns interphase interval elicited a Ca^{2+} transient that was reduced significantly in amplitude compared to that elicited by the unipolar pulse. Increasing the interphase interval to 30 ns elicited Ca^{2+} responses that increased in amplitude to reach a value similar to the one evoked by the unipolar pulse.

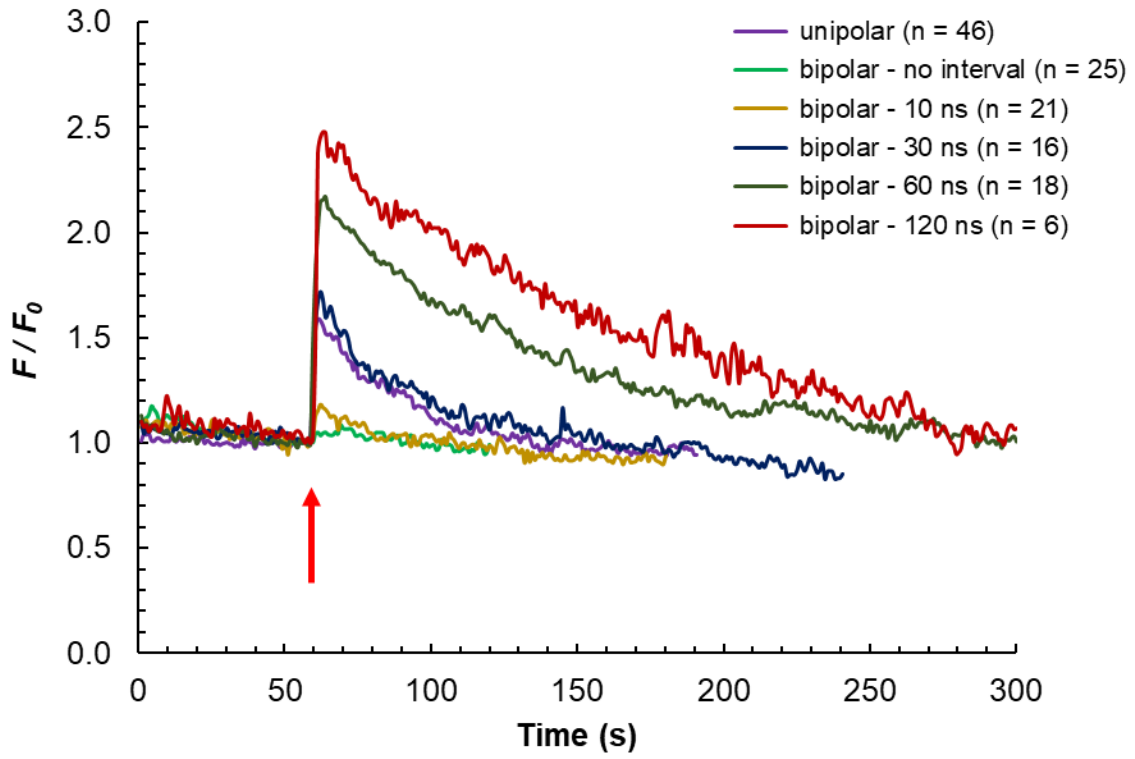

FIGURE S3 Cumulative results of Ca^{2+} responses obtained for different interphase intervals of a 2 ns bipolar pulse. Results are plotted as the averaged fluorescence traces for cells exposed to a 2 ns unipolar pulse or a 2 ns bipolar pulse with various interphase intervals. Representative results are shown in Figure 4 of the manuscript, and these results represent the total number of experiments performed. The number of cells tested are: n = 46 for the unipolar pulse (light blue trace), n = 25 (dark blue trace), 21 (orange trace),

16 (green trace), 18 (red trace) and 6 (purple trace) cells for bipolar pulses with no interphase interval, 10, 30, 60 and 120 ns interphase intervals, respectively. The arrow indicates the time of pulse delivery.